

Ab initio modeling of the structural, electronic, and optical properties of $A^{II}B^{IV}C_2^V$ semiconductors

V. L. Shaposhnikov,* A. V. Krivosheeva, and V. E. Borisenko

Belarusian State University of Informatics and Radioelectronics, P. Browka 6, 220013 Minsk, Belarus

J.-L. Lazzari and F. Arnaud d'Avitaya

*Centre Interdisciplinaire de Nanoscience de Marseille, CINaM, UPR CNRS 3118 conventionnée à Aix-Marseille Université, Case 913,**Campus de Luminy, 13288 Marseille cedex 9, France*

(Received 4 December 2010; published 1 May 2012)

The structural, electronic, and optical properties of $II-IV-V_2$ ($II = Be, Mg, Zn, Cd$; $IV = Si, Ge, Sn$; $V = P, As$) chalcopyrite-type ternaries have been theoretically investigated from first principles. The compounds demonstrate semiconducting behavior, with the direct-band gap ranging from about 0.2 to 2.2 eV, except for Be-containing materials, which indicate an indirect gap. The band gaps in $II-IV-P_2$ are always larger than corresponding ones in $II-IV-As_2$. All compounds are characterized by similar optical spectra with some anisotropy effects. $MgGeAs_2$, $MgSnP_2$, $MgSnAs_2$, $ZnSiAs_2$, $ZnGeP_2$, $ZnSnP_2$, $CdSiAs_2$, and $CdGeP_2$ were found to have the dipole matrix element of the first direct transition comparable with one for GaAs, that may be useful in light-emitting structures. $ZnSiAs_2$, $ZnSnAs_2$, and their solid solutions seem to be the most promising candidates for photovoltaic applications because of their reflectance and absorption spectra.

DOI: [10.1103/PhysRevB.85.205201](https://doi.org/10.1103/PhysRevB.85.205201)

PACS number(s): 71.20.Nr, 78.20.Bh, 71.15.Mb

I. INTRODUCTION

There are two main aspects of interest for a material to be used in optoelectronics: emission of light and photoelectric or photovoltaic effect.¹ A compound for a light source (such as light-emitting or laser diode) should be a direct-gap semiconductor having significant oscillator strength of the first direct transition. The wavelength of the light, and therefore its color, depends on the band-gap energy of the materials forming the $p-n$ junction. For example, GaAs is used in devices working in red and infrared spectral regions.¹ As the sun is the most abundant and reliable source of energy,² photoelectric solar energy converters are currently attracting special attention. For solar cells, a material should possess a high absorption coefficient and thereby should have a direct gap preferably large enough (close to 1.4 eV) to absorb light of the visible spectrum.³

Until recently, the high cost and low efficiency of solar cells have restrained their wide use in daily life. However, new materials suitable for photovoltaics have become the object of investigation together with the new technology of solar cell fabrication. The most used materials for photovoltaic applications are amorphous or crystalline silicon and cadmium telluride (CdTe), as well as $I-III-VI_2$ chalcogenides.¹ In the past few years, the latter semiconductors have been intensively studied, with a special attention paid to $CuInSe_2$ (band gap of about 1.0 eV), which is already used for high-efficient solar cells due to its high ability to absorb light.⁴ This compound can easily be obtained by means of electrochemical deposition and is used mostly in the form of solid solution with $CuGaSe_2$ (which has a band gap of about 1.7 eV) for thin-film solar cells having an efficiency up to 20%.⁵

Meanwhile, it is interesting to find other materials with similar properties that at the same time have an optimal band gap for higher effectiveness of possible devices. One such alternative may be $II-IV-V_2$ compounds, which are ternary analogs of $III-V$ binaries, when the group III element is replaced by the elements of groups II and IV. In most

$III-V$ semiconductors, such replacement leads to a distorted $1 \times 1 \times 2$ supercell of the sphalerite structure, known as a chalcopyrite structure, the same as for $CuInSe_2$. In such structures, the c/a lattice parameters ratio is usually slightly different from 2, and the distortion parameter u differs from the ideal $1/4$ value, which could provide new fundamental electronic, transport, and optical properties of the materials because of the symmetry lowering and different arrangements of cations.⁶ Semiconductors of $II-IV-V_2$ class are numerous when taking into account the choice of II, IV, and V elements. Nevertheless, when choosing compounds appropriate for certain needs, one may restrict all the variety to several materials. For photovoltaic applications, we are interested in stable compounds with an enthalpy of formation less than -1 eV, and thus we may eliminate many N- or C-based materials.^{7,8} The compounds with Zn or Cd at the II type atom position are the most investigated materials, both theoretically and experimentally.^{9,10} In contrast to them, there are only few papers devoted to Mg-containing chalcopyrites (with $MgSiP_2$ as the only investigated one), and no experimental data are available for $Be-IV-V_2$ compounds, while theoretical simulation finds them interesting for spintronics due to their magnetic properties obtained by doping with $3d$ transition metals.^{11,12}

In our work, we focus on $II-IV-V_2$ ($II = Be, Mg, Zn, Cd$; $IV = Si, Ge, Sn$; $V = P, As$) materials and present the results of *ab initio* calculations of their structural, electronic, and optical properties within the density functional theory.

II. COMPUTATIONAL DETAILS

Following to the experimental data, we consider hereby $II-IV-V_2$ ternary compounds in body-centered tetragonal (*bct*) chalcopyrite structure (space group $I\bar{4}2d$) with 8 atoms in the unit cell, the lattice constant a corresponding to the lattice constant of a cubic zincblende structure, the c/a ratio, and the internal displacement parameter u revealing the distortion of the anion sublattice due to different surroundings. In the ideal structure, $c/a = 2$ and $u = 1/4$. The lattice constants together

with the appropriate atomic positions were optimized in the relaxation process, and the resulting equilibrium structural parameters were obtained.

The full structural optimization was performed using the Vienna *ab initio* simulation package (VASP) with a plane-wave basis-set and ultrasoft pseudopotentials.^{13,14} Exchange and correlation potentials were included using the generalized gradient approximation (GGA) of Perdew, Burke, and Ernzerhof.¹⁵ Total energy minimization was obtained by calculating Hellmann-Feynman forces and the stress tensor. The optimization of lattice parameters and the relaxation of atomic positions have been done by the conjugate gradient method. The atomic relaxation was stopped when forces acting on atoms were less than 0.01 eV/Å. The Brillouin zone (BZ) integration was performed by the linear tetrahedron method with Blöchl corrections.¹⁶ An energy cutoff of 330 eV was applied, while the $10 \times 10 \times 10$ grid of Monkhorst-Pack points was used. The convergence in the total energy of the unit cell was better than 1 meV/atom. To find more accurate band gap values and densities of states (DOS) spectra, we applied GW_0 approximation,¹⁷ where only the eigenvalues in the Green's function G are updated until self-consistency is reached. That allows us to obtain better agreement with experiments than a GW approximation in which the eigenvalues in the Green's function G and the screened operator W are updated.

Energy band structures and optical properties of II–IV– V_2 chalcopyrite compounds were calculated by the full-potential linearized augmented plane wave (FLAPW) method (WIEN2K package)¹⁸ with the same GGA parameterization.¹⁵ The structural parameters of the compounds fully optimized by VASP were used. The corresponding plane-wave cutoff $R_{MT} \cdot K_{\max}$ was kept equal to 8 for all cases considered. Expansion up to $l = 10$ in the muffin-tin (MT) spheres was applied. The nonoverlapping MT spheres of maximal possible radii R_{MT} were used. The self-consistent procedure was performed on the $10 \times 10 \times 10$ grid of \mathbf{k} -points uniformly distributed in the irreducible part of the *bct* BZ. Further increase in the cutoff value and \mathbf{k} -point number did not lead to any noticeable changes in the eigenvalues. The self-consistent procedure was continued until the difference between the total energies in two successive iterations was less than 1 meV/atom. For the band structure representation, we have chosen up to 30 \mathbf{k} -points for each segment along the high-symmetry directions. A dense $14 \times 14 \times 14$ grid of \mathbf{k} -points was used to estimate the dipole matrix element that is the key for optical spectra. The interband contribution to the imaginary part of the dielectric function (ϵ_2) was computed within the random-phase approximation, neglecting local-field and finite-lifetime effects. The Kramers-Kronig relation was applied to obtain the corresponding real part (ϵ_1). We also applied the modified Becke-Johnson (mBJ) exchange-correlation potential, which has proven to be a promising tool for accurate determination of the fundamental band gaps of wide-band-gap insulators, *sp* semiconductors, and transition-metal oxides.¹⁹

For comparison reasons, the electronic and optical properties of the most studied representatives of III–V semiconductors (GaAs and GaP) together with some I–III–VI₂ chalcopyrites were calculated using the same computational procedure.

III. RESULTS AND DISCUSSION

A. Structural properties

Our results of the crystal structure optimization of II–IV– V_2 compounds are summarized in Table I. The experimental lattice constants and distortion parameter u are taken from the Landolt-Börnstein tables.⁹

Usually GGA overestimates the unit cell volume and lattice constants, which, nevertheless, in our case are in good agreement with the available experimental data. The discrepancy between theory and experiment monotonically increases with lattice constant and reaches a maximum of 2.0% for a lattice constant (CdSnAs₂) and 2.9% for c lattice constant (ZnSnAs₂). For III–V compounds, the linear thermal expansion of the lattice is $4\text{--}5 \times 10^{-6} \text{ K}^{-1}$.⁹ Thus, the discrepancy should not be larger than 0.05–0.2% between 0 K and 300 K, as compared to the obtained 2–3%. The difference between theoretical and experimental c/a ratio is less than 1%.

Analysis of the structural properties shows the following.

Be-containing compounds have a c/a ratio of about 2.0, which slightly increases with increasing lattice constants (both a and c) and decreasing distortion parameter (u) in the row of group IV elements Si–Ge–Sn. At the same time, one may observe an increase of the interatomic distances, in particular, between group II–IV and IV–V atoms. Mg-containing compounds follow the same tendency, except that the increase in the c/a ratio is more pronounced, but it still remains less than 2.0. Similar behavior has been observed for Zn- and Cd-based chalcopyrites, e.g., a monotonic increase in the c/a ratio and both lattice constants (a and c) and a decrease in the distortion parameter (u) with the increase of the atomic number of IV group atoms.

The change of V group atoms from P to As for identical II and IV group elements always leads to an increase of both lattice constants (a and c) by about 3–5%. However, the c/a ratio increases much slower, having a minimum difference of about 0.2% for Be-containing compounds and a maximum difference of about 1.5% for Mg-containing compounds. The distortion parameter in that case decreases by not more than 2%. The increase of the element number of the group IV atoms in the Si–Ge–Sn row always leads to the increase of both lattice constants (by 2–6%) and a sizable decrease of the distortion parameter by up to 11%. The c/a ratio remains practically the same for Be-containing compounds, while it increases up to 5% in case of Mg and about 3% for Zn- and Cd-based chalcopyrites.

Another tendency can be traced when changing the II group atoms in the Be–Mg–Zn–Cd row. An increase of the element number leads to an increase of both a and c lattice constants. The exception is for Zn-based compounds, for which lattice constants are lower in comparison with Mg-containing ones. The interatomic distance between group IV and V atoms remains practically constant with the change of group II atoms. The same situation is observed for the interatomic distance between group II and V atoms, which does not depend on the group IV atoms.

The lattice constants of II–IV– V_2 chalcopyrites for different group IV elements are plotted in Fig. 1.

These results allow us to assume that BeXAs₂ and ZnXP₂ compounds ($X = \text{Si, Ge}$) are suitable for silicon substrates,

TABLE I. The theoretical (th) and experimental (exp) lattice constants, c/a ratio, distortion parameter (u), and interatomic distances (d) for II–IV–V₂ compounds compared to some I–III–VI₂ and III–V compounds. The theoretical structural parameters were obtained by GGA calculations. The experimental lattice constants are taken from Landolt-Börnstein tables.⁹

Compound	a^{th} (Å)	c^{th} (Å)	$(c/a)^{th}$	a^{exp} (Å)	c^{exp} (Å)	$(c/a)^{exp}$	u^{th}	$d(\text{II–IV})$ (Å)	$d(\text{II–V})$ (Å)	$d(\text{IV–V})$ (Å)
BeSiP ₂	5.121	10.217	1.995	–	–	–	0.235	3.617	2.172	2.262
BeSiAs ₂	5.360	10.711	1.998	–	–	–	0.231	3.789	2.262	2.382
BeGeP ₂	5.205	10.451	2.008	–	–	–	0.221	3.680	2.172	2.348
BeGeAs ₂	5.439	10.945	2.012	–	–	–	0.218	3.846	2.264	2.465
BeSnP ₂	5.423	10.907	2.011	–	–	–	0.195	3.835	2.195	2.536
BeSnAs ₂	5.644	11.369	2.014	–	–	–	0.194	3.991	2.283	2.644
MgSiP ₂	5.733	10.242	1.787	5.720	10.120	1.769	0.292	3.844	2.549	2.261
MgSiAs ₂	5.954	10.800	1.814	–	–	–	0.286	4.019	2.633	2.380
MgGeP ₂	5.787	10.740	1.856	–	–	–	0.278	3.947	2.546	2.355
MgGeAs ₂	6.009	11.270	1.876	–	–	–	0.273	4.119	2.632	2.471
MgSnP ₂	5.923	11.586	1.956	–	–	–	0.251	4.143	2.550	2.543
MgSnAs ₂	6.138	12.057	1.964	–	–	–	0.249	4.302	2.637	2.648
ZnSiP ₂	5.425	10.552	1.945	5.400	10.438	1.933	0.269	3.784	2.389	2.269
ZnSiAs ₂	5.666	11.051	1.951	5.606	10.886	1.942	0.264	3.957	2.479	2.389
ZnGeP ₂	5.502	10.850	1.972	5.463	10.740	1.966	0.254	3.863	2.385	2.358
ZnGeAs ₂	5.742	11.398	1.985	5.671	11.153	1.967	0.251	4.045	2.482	2.479
ZnSnP ₂	5.695	11.476	2.015	5.652	11.305	2.000	0.229	4.027	2.404	2.544
ZnSnAs ₂	5.920	12.043	2.034	5.852	11.703	2.000	0.227	4.186	2.503	2.658
CdSiP ₂	5.731	10.554	1.842	5.679	10.431	1.837	0.297	3.895	2.588	2.268
CdSiAs ₂	5.977	11.077	1.853	5.885	10.881	1.849	0.290	4.074	2.676	2.391
CdGeP ₂	5.811	10.976	1.889	5.740	10.776	1.877	0.283	3.996	2.587	2.364
CdGeAs ₂	6.055	11.483	1.897	5.943	11.220	1.888	0.278	4.172	2.679	2.483
CdSnP ₂	5.986	11.714	1.957	5.901	11.514	1.951	0.257	4.188	2.599	2.548
CdSnAs ₂	6.212	12.182	1.961	6.089	11.925	1.958	0.254	4.350	2.688	2.658
								$d(\text{I–III})$ (Å)	$d(\text{I–VI})$ (Å)	$d(\text{III–VI})$ (Å)
CuInSe ₂	5.862	11.792	2.012	5.780	11.550	1.998	0.220	4.145	2.447	2.648
CuInS ₂	5.576	11.251	2.018	5.520	11.080	2.007	0.223	3.943	2.337	2.513
CuGaSe ₂	5.665	11.232	1.983	5.610	11.000	1.961	0.247	3.989	2.435	2.458
CuGaS ₂	5.368	10.601	1.975	5.350	10.460	1.955	0.251	3.772	2.317	2.312
									$d(\text{III–V})$ (Å)	
GaAs	5.723	–	–	5.654	–	–	0.25	–	2.478	–
GaP	5.492	–	–	5.451	–	–	0.25	–	2.378	–

while ZnXAs₂ (X = Si, Ge) or XSiP₂ (X = Mg, Cd) compounds are closely matched to GaAs lattice.

B. Electronic properties

The band gap values of II–IV–V₂ compounds estimated with different techniques in comparison with available experimental data together with dipole matrix element values of the first direct transition are presented in Table II. The experimental band gaps are taken from the Landolt-Börnstein tables,⁹ except the data for some Be- and most of Mg-containing compounds, for which E_g is taken from theoretical predictions.^{7,10,20,21}

The total DOS as well as the electronic band spectra for the isostructural ternary compounds demonstrate all compounds to be semiconductors.

1. Density of states

To understand the nature of the interatomic interactions in the investigated compounds, the projected DOS spectra

calculated by mBJ are presented in Fig. 2 for the example of ZnGeAs₂ and its binary analog GaAs. The low-lying valence bands ranging from about -9.0 to -6.0 eV are composed mainly of localized d states of group II atoms (for Cd or Zn), s states of group IV atoms, and s and p states of group V atoms. The valence bands, ranging from about -6.0 eV up to the Fermi level, are formed mainly by the interaction of p orbitals of group IV atoms with p orbitals of group V atoms and some admixture of p orbitals of group II atoms.

The conduction bands near the Fermi level are composed mainly of p orbitals of group IV and V atoms, which strongly interact. Moreover, the partial DOS spectra of Ge- $3s$ states practically coincide with those of As- $4p$ ones in the energy region 0 – 2.5 eV. That implies that the strong interaction between group IV and V atoms is highly covalent.

Similar behavior of the total and partial DOS has been observed for GaAs. Here, the valence bands near the Fermi level are composed mainly of $4p$ orbitals of Ga and As atoms, possessing practically the same shape of partial DOS spectra

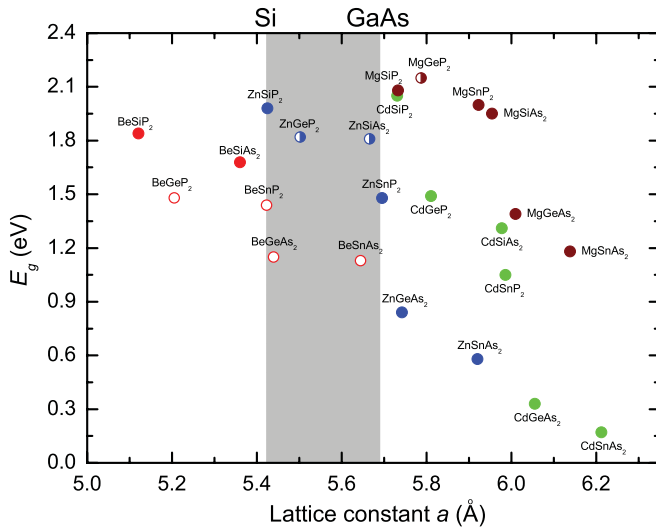


FIG. 1. (Color online) The fundamental band gap calculated by the mBJ potential versus GGA theoretically estimated lattice constant a of II–IV–V₂ chalcopyrites. The filled, unfilled, and half-filled circles correspond to direct-gap, indirect-gap, or quasi-direct-gap compounds, respectively. The shaded areas show the hosts that are expected to be closely ($\pm 2\%$) matched to either Si or GaAs lattices.

as in ZnGeAs₂. The lowest conduction bands are formed by $4p$ states of Ga hybridized with $4p$ states of As. Here, the Ga- $4s$ curve practically repeats the shape of the As- $4p$ one up to about 4 eV.

Thus, the d orbitals of II group atoms (if they exist) do not greatly influence the band gap character in chalcopyrite type II–IV–V₂ semiconductors because these orbitals are highly localized and form valence bands far from the Fermi level.

Quite different regularities were observed for CuInSe₂, in which $3d$ states of Cu form the valence bands in the range from -2 eV to 0 eV below the Fermi level.

2. Band structures

In the small energy range near the Fermi level, the energy spectra of all considered chalcopyrite compounds are practically similar. The shape of the highest valence and lowest conduction bands repeats the ones in GaAs.

The electronic energy band structures of several chalcopyrite compounds having the most striking features (direct band gap and sizable value of the dipole matrix element of the first direct transition at the Γ point) are presented in Fig. 3. The band spectra were calculated by mBJ along some high-symmetry directions of BZ. The reciprocal coordinates for the \mathbf{k} -points of the bct BZ used are the following: T = $2\pi/c \cdot (0, 0, 1)$, $\Gamma = (0, 0, 0)$, and N = $2\pi/a \cdot (1/2, 1/2, 0)$.

Most of the chalcopyrite compounds considered are found to be direct-gap semiconductors with the gaps located at the Γ -point. According to our theoretical predictions, the gap values range from about 0.1 to 1.5 eV (GGA), 0.17 to 2.15 eV (mBJ), and 0.16 to 2.28 eV (GW_0) (see Table II). It has been found that the band gap values obtained by GGA are always smaller than those estimated with the mBJ or GW_0 techniques. However, as it will be shown in further discussion, all the methods used reproduce the main features of the electronic and optical spec-

tra correctly. Thus, herein we will use the results of the mBJ calculations.

Among Be-containing materials, only two of them (namely BeSiP₂ and BeSiAs₂) are direct-gap semiconductors, whereas the others are characterized by an indirect energy gap with the valence band maximum (VBM) still located at the center of the BZ, but where the conduction band minimum (CBM) is shifted from the Γ -point along the Γ -T direction. The indirect-gap values are: 1.48, 1.15, 1.44, and 1.13 eV for BeGeP₂, BeGeAs₂, BeSnP₂, and BeSnAs₂, respectively. Unfortunately, there are no experimental data concerning the electronic properties of Be–IV–V₂ compounds for comparison, while the gaps obtained are in good agreement with theoretical data of Ref. 7, in which the GGA approach was used.

Magnesium-containing compounds are found to be direct-gap semiconductors, except MgGeP₂, which is a quasi-direct-gap semiconductor. Here, the VBM is located at the Γ -point, whereas the CBM at the Γ -point and in the Γ -T direction have practically equal values. For MgSiP₂, the mBJ band gap agrees well with the experimental value, while for other magnesium-containing compounds, our GGA band gaps match with theoretical values.⁷

Zn-containing chalcopyrites are direct-gap semiconductors, except quasi-direct ZnGeP₂ and ZnSiAs₂, in which the VBM is located at the Γ -point, whereas the CBM values at the Γ - and N-points have practically equal energy values. The band spectra and energy gaps obtained by GGA are in good agreement with available theoretical predictions.^{7,22} In the latter work, the linear muffin-tin orbitals (LMTO) method within local density approximation (LDA) was used. Also, GW_0 and mBJ band gaps are closer to experimental data, while GGA ones sizably underestimated gap values, especially for ZnXAs₂ (X = Ge, Sn).

As found by mBJ calculations, all of Cd–IV–V₂ compounds considered possess direct band gaps. GGA calculations have reported CdGeAs₂ and CdSnAs₂ to be practically gapless, whereas, experimentally, they have band gaps of 0.57 and 0.26 eV, respectively.

The common tendencies for the band gaps of the studied chalcopyrite compounds are the following: the energy gaps for P-containing compounds are larger as compared with As-containing ones. A similar trend can be traced for III–V semiconductors: the band gap for GaP is larger than for GaAs.⁹ In the row of IV group atoms (Si, Ge, Sn), the gaps for most Si-containing materials are the largest, and gaps for corresponding Sn-containing ones are the smallest. This can be connected with the lattice constants and atomic radii of the corresponding elements.

It is well-known that methods within the density functional theory that do not use the electronic self-energy corrections usually underestimate band gap values with respect to the ones derived from experiments. To clarify this situation in application to chalcopyrite-type semiconductors, some partial DOS spectra near the Fermi level for MgSiP₂ calculated by mBJ, GGA, and GW_0 techniques are presented in the Fig. 4.

It is obvious that GW_0 and mBJ represent all of the main peaks and features of partial DOS spectra, as GGA does. However, the broadening of both valence and conduction bands spectra can be observed in the case of GW_0 and mBJ. The value is different for various materials; moreover, the

TABLE II. The experimental (exp) energy band gaps (E_g) compared to theoretical ones as calculated within GGA, mBJ, and GW_0 approximations and dipole matrix element ($|P|^2$) of the first direct transition at the Γ -point for II–IV–V₂ and some I–III–VI₂ and III–V compounds. The symbols (d), (qd), and (i) are used for direct, quasi-direct, or indirect gaps, respectively.

Compound	E_g^{GGA} (eV)	E_g^{mBJ} (eV)	$E_g^{GW_0}$ (eV)	E_g^{exp} (eV)	$ P ^2$
BeSiP ₂	1.20 (d)	1.84	1.75	1.3 ^c	0
BeSiAs ₂	1.07 (d)	1.68	1.33	1.1 ^c	0
BeGeP ₂	0.85 (d)	1.48	1.58	0.9 ^c	0
BeGeAs ₂	0.62 (i)	1.15	1.07	1.68 ^b	0
BeSnP ₂	0.91 (i)	1.44	1.78	1.98 ^b	0
BeSnAs ₂	0.68 (i)	1.13	1.25	1.15 ^b	0.112 Px
MgSiP ₂	1.37 (d)	2.08	1.83	2.0, 2.26	0
MgSiAs ₂	1.26 (d)	1.95	1.40	2.0 ^d , 2.08 ^a , 2.67 ^b	0
MgGeP ₂	1.52 (qd)	2.15	2.28	2.1 ^d , 2.17 ^a , 3.0 ^b	0
MgGeAs ₂	0.57 (d)	1.39	1.27	1.6 ^{a,d} , 2.18 ^b	0.209 Pz
MgSnP ₂	1.20 (d)	2.00	2.05	1.56 ^a , 1.8 ^d , 2.48 ^b	0.174 Pz
MgSnAs ₂	0.42 (d)	1.18	1.07	0.93 ^a , 1.2 ^d , 1.65 ^b	0.185 Pz
ZnSiP ₂	1.38 (d)	1.98	1.92	2.0–2.3	0
ZnSiAs ₂	0.89 (qd)	1.81	1.94	1.6–1.8	0.277 Pz
ZnGeP ₂	1.16 (qd)	1.82	2.25	1.8–2.2	0.234 Pz
ZnGeAs ₂	0.10 (d)	0.84	0.80	1.15	0
ZnSnP ₂	0.66 (d)	1.48	1.68	1.5–1.7	0.106 Px
ZnSnAs ₂	0.10 (d)	0.58	0.47	0.75	0
CdSiP ₂	1.42 (d)	2.05	1.91	2.2–2.45	0
CdSiAs ₂	0.38 (d)	1.31	1.29	1.55	0.242 Pz
CdGeP ₂	0.59 (d)	1.49	1.61	1.72	0.213 Pz
CdGeAs ₂	0.10 (d)	0.33	0.26	0.57	0
CdSnP ₂	0.23 (d)	1.05	1.10	1.17	0.189 Pz
CdSnAs ₂	0.05 (d)	0.17	0.16	0.26	0
CuInSe ₂	0.05 (d)	0.31	0.41	1.0–1.3	0
CuInS ₂	0.03 (d)	0.54	0.47	1.53	0
CuGaSe ₂	0.11 (d)	0.82	2.58	1.68–1.96	0.113 Pz
CuGaS ₂	0.80 (d)	1.41	1.74	2.43	0.080 Pz
GaAs	0.35 (d)	1.21	1.30	1.42–1.52	0.104
GaP	1.66 (i)	2.33	2.60	2.26	0.085

^aReference 20;

^bReference 21;

^cReference 7;

^dReference 10.

shift of the peaks in the conduction band is higher than that in the valence band. That leads to band gap enlargements. The comparison of the theoretical band gaps of II–IV–V₂ compounds with available experimental data (see Table II) shows that, in most cases, both GW_0 approximation and mBJ exchange-correlation potential allow prediction of band gap values much more closer to experimental values than usual GGA calculations. Thus, the optical properties spectra presented next were calculated within mBJ.

C. Optical properties

Real and imaginary parts of the dielectric function were calculated along two main crystallographic directions in the energy region of 0–10 eV. The squared values of the dipole matrix elements $|P|^2$ (presented in Table II) of the interband direct transitions at the Γ -point between upper valence bands (which are degenerated at the Γ -point) and the

lower conduction band were calculated and compared with those of III–V compounds (GaAs and GaP). A material with large $|P|^2$ and a direct band gap may be used as a light-emitting compound. In order to estimate the usefulness and applicability of II–IV–V₂ chalcopyrite compounds for photovoltaics, the averaged reflection and absorption spectra were calculated in the visible range. The most representative results are shown below.

Optical spectra of Be-containing compounds (Fig. 5) are characterized by equal starts and practically the same shape of ε_2 curves for both directions of light polarization. Some differences can be found at higher photon energies (about 5 eV), indicating the slightly different location of the main peaks for $E\parallel a$ and $E\parallel c$ (for BeSiP₂) or at about 3 eV showing different amplitudes of peaks (for BeGeAs₂). BeSiP₂ and BeSiAs₂ are found to be direct-gap semiconductors; moreover, they are characterized by the rapid increase of ε_2 curves at about 3.0 eV, which can be explained by the transitions

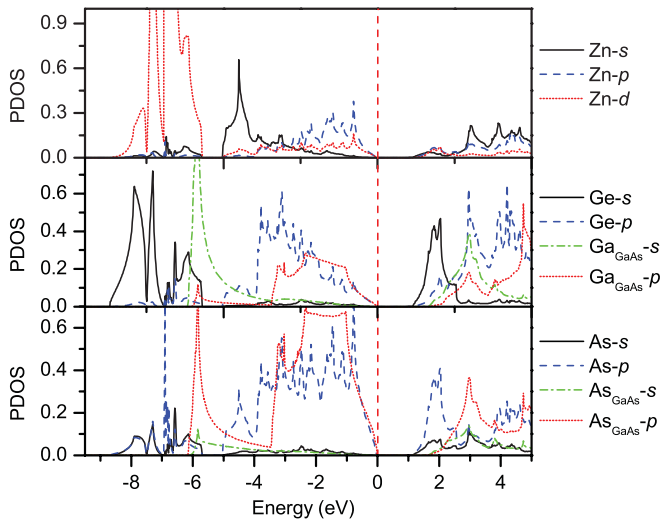


FIG. 2. (Color online) The projected DOS (states/eV/cell) of ZnGeAs₂ compared with ones of GaAs as calculated by the mBJ potential. Zero at the energy scale corresponds to the Fermi level.

between more distant bands. That is confirmed by the analysis of dipole matrix elements of the first across-gap transition at the Γ -point, which are practically zero for both compounds considered. The only material among Be-IV-V₂ compounds with a sizable dipole matrix element of the first direct transition at the Γ -point is BeSnAs₂ ($|P_{xx}|^2 = 0.112$ for $E\parallel a$), which is proved by the first peak of the ϵ_2 spectrum along the x direction. However, that material is characterized by an indirect band gap.

The dielectric functions of Mg-compounds (Fig. 6) show more anisotropic behavior, especially for the photon energies higher than 4 eV. Both Si-containing direct-gap compounds are characterized by a low dipole matrix element of the first direct

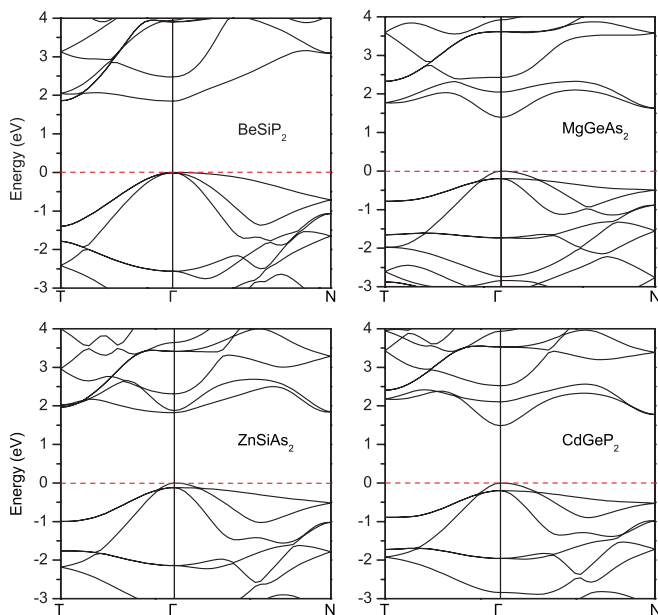


FIG. 3. (Color online) The mBJ band structures of II-IV-V₂ compounds along some high-symmetry directions of the *bct* BZ. The zero level corresponds to the Fermi level.

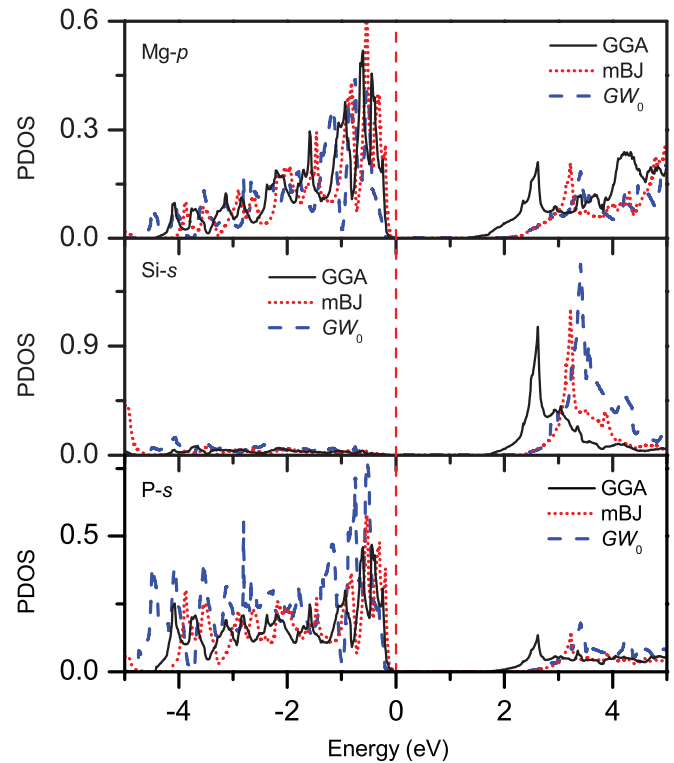


FIG. 4. (Color online) The projected DOS (states/eV/cell) of MgSiP₂ calculated within GGA, mBJ, and GW_0 . Zero at the energy scale corresponds to the Fermi level.

transition, as well as MgGeP₂. MgGeAs₂ is found to have a large value of the dipole matrix element (0.209 for $E\parallel c$), and its ϵ_2 spectra are characterized by an abrupt threshold and a strong increase at about 1.4 eV, which corresponds to the value of the estimated band gap. Both Sn-containing direct-gap compounds also have $|P_{zz}|^2$ comparable to GaAs: 0.174 for MgSnP₂ and 0.185 for MgSnAs₂. Their ϵ_2 spectra are also characterized by a strong increase at about 2.0 eV (for MgSnP₂) and 1.2 eV (for MgSnAs₂), which are the direct-gap values in these compounds.

The ϵ_2 spectra of Zn-containing materials (Fig. 7) reveal weak anisotropy for photon energies less than 4 eV. The ZnSiAs₂ compound is characterized by a large dipole matrix element (0.277 for $E\parallel c$), and its ϵ_2 spectrum is described by a strong increase at about 1.9 eV. Similar behavior was observed

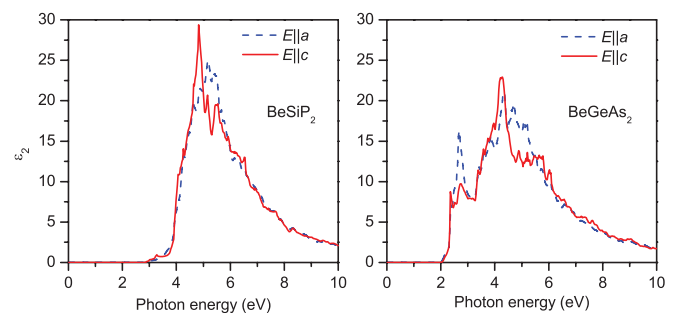


FIG. 5. (Color online) The imaginary part of the dielectric function (ϵ_2) of BeSiP₂ and BeGeAs₂ versus photon energy for different light polarizations as calculated by the mBJ potential.

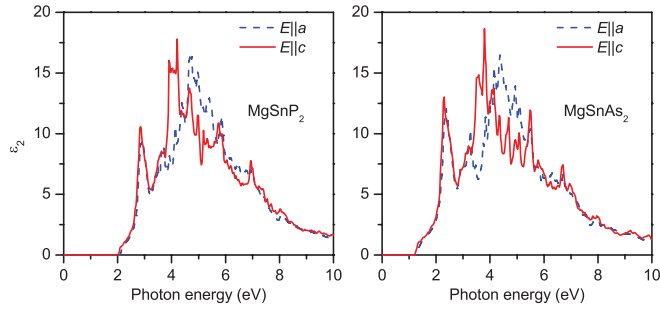


FIG. 6. (Color online) The imaginary part of the dielectric function (ϵ_2) of MgSnP_2 and MgSnAs_2 versus photon energy for different light polarizations as calculated by the mBJ potential.

for ZnGeP_2 ($|P_{zz}|^2 = 0.234$), with the ϵ_2 curve starting at about 2.1 eV in spite of the fact that this compound has a quasi-direct gap. The third compound with valuable $|P_{xx}|^2$ (0.106) is the direct-gap semiconductor ZnSnP_2 .

Cd-based materials provide similar optical properties (Fig. 8) as compared with Zn-based ones. CdSiAs_2 is characterized by a large dipole matrix element (0.242 for $E||c$), and its ϵ_2 spectrum is described by a strong increase at about 1.3 eV. CdGeP_2 has $|P_{zz}|^2 = 0.213$, and its ϵ_2 curve starts at 1.5 eV. For CdSnP_2 the ϵ_2 spectra begins at about 1.05 eV for $E||c$, while $|P_{zz}|^2 = 0.189$. Narrow-gap compounds CdGeAs_2 and CdSnAs_2 have $|P|^2 = 0$.

The common feature of the imaginary parts (ϵ_2) of the dielectric function is that the energy of their starting points decreases in the row Si–Ge–Sn for all II–IV–V₂ chalcopyrites considered. The calculated real parts of the dielectric function (ϵ_1) reproduce all the features of the corresponding ϵ_2 spectra. The static dielectric function $\epsilon_1(0)$ remains practically the same for both light polarizations, ranging from 10 to 20 for different studied materials. It was found to be slightly higher for As-containing compounds than those having P as group V atoms.

The similarity of the optical spectra of chalcopyrite compounds with their binary analogues shows close relation between their energy band structures. Thus, the principal peaks in the ϵ_2 spectra of II–IV–V₂ compounds are concluded to be mainly caused by optical transitions in chalcopyrite Brillouin zone, which have been derived from the direct transitions in

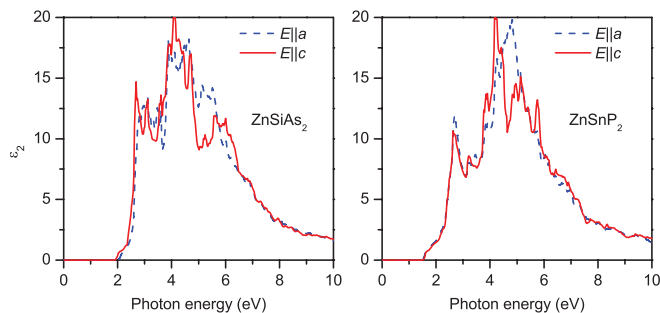


FIG. 7. (Color online) The imaginary part of the dielectric function (ϵ_2) of ZnSiAs_2 and ZnSnP_2 versus photon energy for different light polarizations as calculated by the mBJ potential.

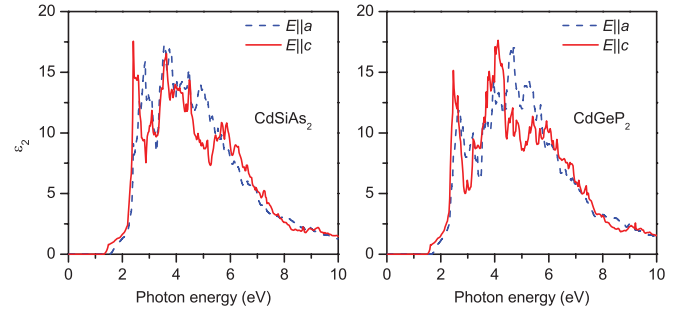


FIG. 8. (Color online) The imaginary part of the dielectric function (ϵ_2) of CdSiAs_2 and CdGeP_2 versus photon energy for different light polarizations as calculated by the mBJ potential.

sphalerite and are responsible for the basic features in the optical spectra of the III–V semiconductors.

The band gap E_g of a semiconductor defines the minimum energy value of photons absorbed. To be used in photovoltaics, a material should satisfy some requirements: to be a direct-gap semiconductor, and to have a sizable band gap value (more than 1.2 eV), small reflectance, and large absorption coefficient to absorb the essential part of the visible light spectrum.³ However, the compound with a band gap higher than 1.5 eV may absorb less of visible spectrum. The calculated reflectance spectra, averaged over both directions of light polarization for some of II–IV–V₂ chalcopyrites compared to the most investigated representatives of III–V semiconductors (GaAs and GaP) and I–III–VI₂ chalcopyrites (CuInSe_2), are presented in Fig. 9.

Obviously, the reflectivity of II–IV–V₂ compounds is about two times higher than that of CuInSe_2 in the visible range, but it is comparable with GaAs and GaP ones.

The calculated absorption coefficients averaged over directions of light polarization for some of II–IV–V₂ chalcopyrite compounds are presented in Fig. 10 in comparison with GaAs, GaP, and CuInSe_2 materials.

Among Be-containing compounds, only BeGeAs_2 and BeSnAs_2 are characterized by high absorption coefficients; however, both of them are indirect-gap semiconductors.

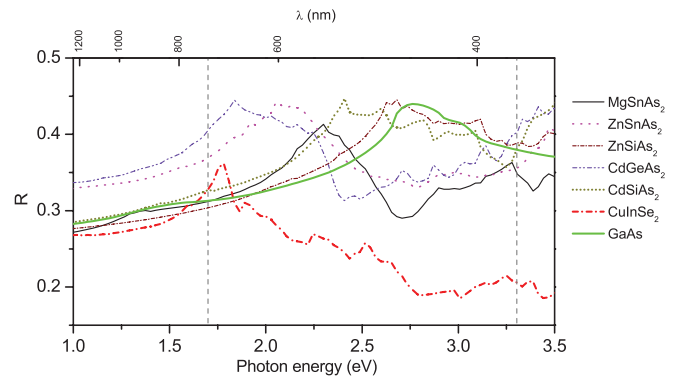


FIG. 9. (Color online) The averaged reflectance spectra of some II–IV–V₂ ternary compounds in comparison with those of CuInSe_2 and GaAs materials as calculated by the mBJ potential. Vertical dashed lines define the boundaries of the visible spectrum.

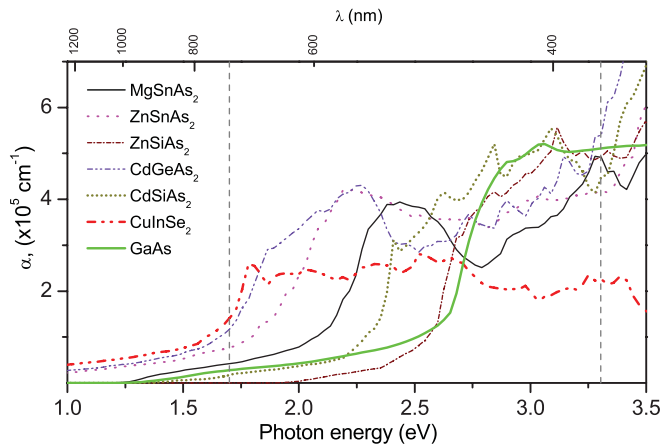


FIG. 10. (Color online) The averaged absorption coefficients of some II–IV–V₂ ternary compounds in comparison with CuInSe₂ and GaAs materials as calculated by the mBJ potential. Vertical dashed lines define the boundaries of the visible spectrum.

MgSiP₂ has the lowest value of the absorption coefficient and a rather large band gap of 2.0 eV, while other Mg–IV–V₂ compounds possess the values comparable with GaAs and GaP. Moreover, the values of α are higher than those for CuInSe₂, especially at photon energies higher than 2.2 eV. Unfortunately, most Be- and Mg-containing compounds (except MgSiP₂) have not been experimentally synthesized and measured, probably because they contain light elements that are not easy to handle: metallic magnesium burns in air and beryllium forms very poisonous compounds. In the group of Zn–IV–V₂ chalcopyrites, ZnSiP₂ has the lowest absorption coefficient at photon energies lower than 2.0 eV, while α for ZnSnAs₂ is about two times higher than for CuInSe₂. CdGeAs₂ and CdSnAs₂ are characterized by satisfactory absorption coefficients; however, their band gaps are rather small. The common tendency is that As-containing compounds possess higher α values than P-containing ones. In the row Si–Ge–Sn, the absorption coefficient for Si-containing materials is the lowest, while Sn-containing chalcopyrites have the largest α values and the smallest band gaps.

Considering practical applicability of materials, the price of the components must also be considered as one of the important factors. From this point of view, expensive Be- and Ge-containing compounds should be replaced by elements of low price to compete with Si, GaAs, CdTe, CdSe, or CuInSe₂. Moreover, it is better not to consider Mg-, Cd-based and P-containing compounds if one wants to eliminate rare, dangerous or too toxic elements. In addition, arsenic compounds are

easier to fabricate in comparison with P-based ternaries. One of the reasonable ways to increase the quantum efficiency of solar cells is to use multijunction (multicolor) heterostructures consisting of semiconducting materials with different band gaps in order to absorb more light of the visible range.^{3,23} As the band gaps in ZnSiAs₂ and ZnSnAs₂ range from about 0.6 to 1.8 eV, these materials look promising for photovoltaics, either in the form of solid-solution ZnSi_{1-x}Sn_xAs₂ or as the heterostructure containing both compounds, due to their lattice constants close to GaAs, large values of optical absorption coefficients in the visible spectrum, and applicable values of the band gap.

IV. CONCLUSIONS

The theoretical study of structural, electronic, and optical properties of II–IV–V₂ (II = Be, Mg, Zn, Cd; IV = Si, Ge, Sn; V = P, As) ternary compounds with chalcopyrite structure performed by means of *ab initio* calculations has revealed the following tendencies: an increase of the atomic number of the group V elements (when group II and IV elements remain the same) always leads to an increase of both lattice constants by about 3–5%; the increase of the atomic number of the group II elements also leads to the increase of both lattice constants, except for Zn-based compounds.

The materials investigated are found to be semiconductors. Most of them possess a direct band gap located at the Γ -point, with the gaps ranging from about 0.2 to 2.2 eV. The band gaps in P-containing compounds are larger than those in As-containing ones; the gaps in II–Si–V₂ materials are higher and in II–Sn–V₂ are smaller when II and V elements are unchanged. Application of modern GW_0 approximation and modified Becke-Johnson exchange-correlation potential to electronic properties calculations of II–IV–V₂ chalcopyrite-type compounds shows good agreement with available experimental data.

An increase of the atomic number of the group IV elements leads to a decrease of the energy of the starting point of the ϵ_2 curve for all chalcopyrites studied. The static dielectric function $\epsilon_1(0)$ remains practically the same for both light polarizations, having the same order of magnitude in these materials. MgGeAs₂, MgSnP₂, MgSnAs₂, ZnSiAs₂, ZnGeP₂, ZnSnP₂, CdSiAs₂, and CdGeP₂ were found to have valuable dipole matrix elements of the first direct transitions that make them promising for light-emission applications. ZnSiAs₂ and ZnSnAs₂ seem to be the most suitable for photovoltaic applications as they have large absorption coefficients, optimal band gaps, and lattice constant of ZnSiAs₂ matched to GaAs substrate.

*Corresponding author: victor.shaposhnikov@gmail.com

¹E. Rosencher and B. Vinter, *Optoelectronics* (Cambridge University Press, Cambridge, UK, 2002).

²A. Luque, *J. Appl. Phys.* **110**, 031301 (2011).

³R. H. Bube, *Photovoltaic Materials* (Imperial College Press, London, 1998), pp. 1–33.

⁴W. N. Shafarman and L. Stolt, in *Handbook of Photovoltaic Science and Engineering*, edited by A. Luque, S. Hegedus (Wiley, Chichester, UK, 2003), pp. 567–616.

⁵M. A. Green, K. Emery, Y. Hishikawa, and W. Warta, *Prog. Photovolt.: Res. Appl.* **18**, 346 (2010).

⁶S. Siebentritt and U. Rau (eds.), *Wide-Gap Chalcopyrites* (Springer, Berlin, Heidelberg, Germany, 2006).

⁷S. C. Erwin and I. Žutić, *Nat. Mater.* **3**, 410 (2004).

⁸V. L. Shaposhnikov, A. V. Krivosheeva, F. Arnaud d’Avitaya, J.-L. Lazzari, and V. E. Borisenko, *Phys. Status Sol. B* **245**, 142 (2008).

⁹Landolt-Börnstein, in *Condensed Matter, Ternary Compounds, Organic Semiconductors, New Series, Group III*, edited by

- O. Madelung, U. Rössler, and M. Schulz, Vol. 41E (Springer-Verlag, Berlin, 2000).
- ¹⁰J. E. Jaffe and A. Zunger, *Phys. Rev. B* **29**, 1882 (1984); **30**, 741 (1984).
- ¹¹A. V. Krivosheeva, V. L. Shaposhnikov, F. Arnaud d'Avitaya, V. E. Borisenko, and J.-L. Lazzari, *J. Phys. Condens. Matter* **21**, 045507 (2009).
- ¹²A. V. Krivosheeva, V. L. Shaposhnikov, V. E. Borisenko, F. Arnaud d'Avitaya, and J.-L. Lazzari, *Proc. SPIE* **7377**, 737705 (2008).
- ¹³G. Kresse and J. Hafner, *Phys. Rev. B* **49**, 14251 (1994).
- ¹⁴G. Kresse and J. Furthmüller, *Comput. Mater. Sci.* **6**, 15 (1996); *Phys. Rev. B* **54**, 11169 (1996).
- ¹⁵J. P. Perdew, K. Burke, and M. Ernzerhof, *Phys. Rev. Lett.* **77**, 3865 (1996).
- ¹⁶P. E. Blöchl, O. Jepsen, and O. K. Andersen, *Phys. Rev. B* **49**, 16223 (1994).
- ¹⁷M. Shishkin and G. Kresse, *Phys. Rev. B* **74**, 035101 (2006); **75**, 235102 (2007).
- ¹⁸P. Blaha, K. Schwarz, G. K. H. Madsen, D. Kvasnicka, and J. Luitz, *WIEN2k, An Augmented Plane Wave + Local Orbitals Program for Calculating Crystal Properties* (Karlheinz Schwarz, Techn. Universität Wien, Vienna, Austria, 2001).
- ¹⁹F. Tran and P. Blaha, *Phys. Rev. Lett.* **102**, 226401 (2009); D. Koller, F. Tran, and P. Blaha, *Phys. Rev. B* **83**, 195134 (2011); A. D. Becke and E. R. Johnson, *J. Chem. Phys.* **124**, 221101 (2006).
- ²⁰Zh. Zhaochun, P. Ruiwu, and C. Nianyi, *Mater. Sci. Eng. B* **54**, 149 (1998).
- ²¹C. Suh and K. Rajan, *Appl. Surf. Sci.* **223**, 148 (2004).
- ²²S. N. Rashkeev, S. Limpijumnong, and W. R. L. Lambrecht, *Phys. Rev. B* **59**, 2737 (1999).
- ²³M. Bosi and C. Pelosi, *Prog. Photovolt: Res. Appl.* **15**, 51 (2007).